Journal of Ship Research, Vol. 45, No. 4, Dec. 2001, pp. 289–301

A Quasi-Explicit Hydrodynamic Model for the Dynamic Analysis of a Moored FPSO Under Current Action

A. N. Simos[*] **E. A. Tannuri,**[†] **C. P. Pesce,**[†] and **J. A. P. Aranha**[*]

[*] *Department of Naval Architecture and Ocean Engineering, USP, S.P., Brazil*
[†] *Department of Mechanical Engineering, USP, S.P., Brazil*

An earlier work Leite et al (1998) developed a heuristic hydrodynamic model, based on the short-wing theory, for the horizontal current forces on an FPSO system. The proposed model was quasi-explicit in the sense that it depends on the ship's main dimensions and on only three hydrodynamic coefficients, namely, the friction coefficient C_f for head on incidence, the drag coefficient C_Y for a cross-flow, and the related yaw moment coefficient lC_Y. As discussed in Leite et al (1998), these coefficients could even be estimated from the ITTC friction curve and from Hoerner's sectional results, which would then turn the hydrodynamic model explicit. The model has been tested against experimental results for the horizontal force coefficients, obtained both at IPT and at the Marin wave tank, and it has also been confronted with bifurcation experiments for a turret configuration realized at IPT. The agreement rendered good results in all cases tested. The heuristic approach has now been extended to incorporate the yaw velocity terms while preserving the quasi-explicit feature of the original model. The main purpose of the work herein is to present such a development together with some experimental validation. Using Froude scaling of different ships in distinct ballast conditions, the horizontal forces and moment in the yaw rotating tests were measured at IPT and at Marin and compared with those predicted by the heuristic model, the observed agreement again being fair enough. In an accompanying paper in this issue, the derived mathematical model is tested against experiments that emulate a single-point mooring of a tanker ship in order to disclose the model's ability to cope with the main dynamic features of the fishtailing instability problem.

1. Introduction

In the analysis of the operations of an FPSO, moored in the open sea, in some cases it is important to predict the horizontal motion of this floating system under environmental action. Steady (and also unsteady) forces caused by wind and wave effects can be determined with some accuracy and in a straightforward manner: Wind forces can be estimated from captive-model tests since only weakly influenced by the FPSO motion, given the enormous difference of velocities between both; wave forces, including the important influence of the wave-current interaction, can be determined from a standard linear frequency-domain program based on potential theory, as discussed, for instance, in Aranha (1996) and Aranha & Martins (2000).

The ocean current effect, however, cannot be uncoupled from the body motion; furthermore, the related forces have both a potential (inertial) and a viscous origin, turning the mathematical prediction awkward, to say the least. In general, these forces are expanded in Taylor's series in the relative velocities and the coefficients of these expansions, the so-called hydrodynamic derivatives, are then obtained from an exhaustive set of experiments. It is certainly not easy to experimentally estimate the higher-order hydrodynamic derivatives and it is not unusual that different laboratories furnish, sometimes, values for these higher-order coefficients that differ not only in modulus but also in sign (see, for example, Kijima (1996)). Even more, if a clear physical model is not defined, it may become difficult to know how to extrapolate

Manuscript received at SNAME headquarters August 9, 2000; revised manuscript received June 1, 2001.

to full-scale the coefficients determined from small-scale physical models. Besides these conceptual problems, there are also some more practical questions that may render this approach unfit to be used in a routine study. In fact, when addressing a real problem where the FPSO is given a certain ballast condition, one faces a dilemma since, almost certainly, one has not at one's disposal experimental results for the particular ship at the specified ballast condition. One might eventually use experimental results derived for a similar ship and try to infer the corresponding hydrodynamic derivatives by interpolation. This approach may fail, however, due mainly to a specific circumstance: The mathematical models for moored ships are prone to develop a variety of dynamically unstable solutions that depending, as they do, on some of the higher-order hydrodynamic derivatives, might not reflect the behavior of the actual system but of the virtual interpolated one.

It seems then desirable to derive a hydrodynamic model with certain features: first, that it has a clear *physical background*, in such a way that the dependence on scale-factors (Reynolds number Re) be well defined; second, that the model be *quasi-explicit*, in the sense that it is a function of some few hydrodynamic coefficients that can be relatively well estimated by standard means; third, that the model be able to adequately reproduce current effects on tanker hulls in the context it was derived for, i.e., the low-velocity limit.

A model aiming such properties is not a novelty in the literature. Clarke et al (1982), for example, applied the short wing theory for a flat plate to derive the structure of the *linear* hydrodynamic derivatives and used a large set of experimental results to obtain, after a statistical analysis, how these derivatives depend on the main ship dimensions. These results have been used by Leite et al (1998)[1] in conjunction with some cross-flow analysis, to derive a quasi-explicit model for the current forces on a FPSO depending only on three hydrodynamic coefficients: the friction coefficient C_f(Re), the cross-flow drag coefficient C_Y, and the related yaw moment lC_Y. The obtained model has been verified by comparing the predicted horizontal forces and moment to those measured experimentally, both at IPT and at Marin, using different ships in distinct ballast conditions. In this case, where the current forces are static in essence, the robustness of the proposed model can be experimentally checked by looking at the static bifurcation phenomenon that occurs in a FPSO in turret configuration: the bifurcation parameter is then the turret position and, from the mathematical model, not only the critical value of this parameter can be predicted and compared to the experiments but also the post-critical behavior, namely, how the equilibrium yaw angle increases as the turret is displaced from its critical position in the direction of more unstable ones.

The agreement between the proposed hydrodynamic model and the experiments, both for the horizontal forces and moment and also for the more acute and sensible bifurcation phenomenon, is good, showing that the proposed model can be confidently used at least to study the static configurations of a moored FPSO. The intention of the present work is to extend the former model by incorporating the dynamic parcels related to the yaw velocity terms, while preserving its original simplicity. Such a development is made in Section 2, where the physical background is also described, and in Section 3 the influence of the yaw velocity terms on the horizontal forces and moment is verified against experimental results conducted at IPT and Marin, for different ships in distinct ballast conditions. In order to assess the robustness of the proposed model, in the context of moored ships, the crucial test seems to be the model's performance in describing the fishtailing instability that usually occurs for a single-point mooring system. It is thus important to check not only the model's ability in detecting the threshold point but also in predicting the amplitude and period of the related limit-cycle. This problem, however, has some important particularities, mainly on the experimental side, being more suitable to be discussed in a companion paper.

[1] As it has been pointed out to the authors, the model derived by Oltmann & Sharma (1984) is very similar to the one independently obtained by Leite et al (1998).

2. Hydrodynamic model

Let $(O; x, y, z)$ be the local coordinated axis, the x-axis being in the longitudinal direction towards the bow, the y-axis in the port direction and the z-axis in the vertical direction, pointing upwards; the origin O is assumed to be at the ship's midsection. Let also $(u(t), v(t))$ be the components of the ship velocity with respect to the water and $r(t)$ be the yaw angular velocity. In this paper M is the displaced mass, I_Z the moment of inertia with respect to the z-axis and x_G the longitudinal position of the center of gravity; the fluid inertia tensor is defined by $\{M_{ij}; i, j = 1, 2, \ldots 6\}$ with $i = 1$ for the surge motion, $i = 2$ for the sway motion and $i = 6$ for the yaw angular displacement. The equations of motion in the horizontal plane are given by

$$\begin{aligned}
&(M + M_{11})\dot{u} - (M + M_{22})vr - (Mx_G + M_{26})r^2 \\
&\qquad = F_{X,R}(u, v, r) + F_X \\
&(M + M_{22})\dot{v} + (Mx_G + M_{26})\dot{r} + (M + M_{11})ur \\
&\qquad = F_{Y,R}(u, v, r) + F_Y \\
&(I_Z + M_{66})\dot{r} + (Mx_G + M_{26})\dot{v} + (M_{22} - M_{11})uv - (Mx_G + M_{26})ur \\
&\qquad = N_{Z,R}(u, v, r) + N_Z
\end{aligned} \tag{1}$$

with $\{F_{X,R}(u, v, r); F_{Y,R}(u, v, r); N_{Z,R}(u, v, r)\}$ being generalized fluid forces, mainly of rotational origin, and $\{F_X; F_Y; N_Z\}$ being the remaining generalized forces due to wind, wave and geometric constraints eventually imposed to the FPSO. The generalized fluid forces $\{F_{X,R}(u, v, r); F_{Y,R}(u, v, r); N_{Z,R}(u, v, r)\}$ can also be expressed in the form

$$\begin{aligned}
F_{X,R}(u, v, r) &= F_{X,R}(u, v, 0) + \Delta F_{X,R}(u, v, r); \\
&\qquad \Delta F_{X,R}(u, v, r)\big|_{r=0} = 0 \\
F_{Y,R}(u, v, r) &= F_{Y,R}(u, v, 0) + \Delta F_{Y,R}(u, v, r); \\
&\qquad \Delta F_{Y,R}(u, v, r)\big|_{r=0} = 0 \\
N_{Z,R}(u, v, r) &= N_{Z,R}(u, v, 0) + \Delta N_{Z,R}(u, v, r); \\
&\qquad \Delta N_{Z,R}(u, v, r)\big|_{r=0} = 0
\end{aligned} \tag{2}$$

and it is aimed, next, to obtain convenient expressions for these force components.

Sway and surge components $(r = 0)$

Consider the floating body moving with velocity $u\mathbf{i} + v\mathbf{j}$ through the fluid and let

$$U = \sqrt{u^2 + v^2}$$
$$\alpha = \pi + \arctan(v/u) \tag{3}$$

In the reference system moving with the body one sees a current with intensity U incident in a direction that makes an angle α with the longitudinal axis. Using the expressions derived in Leite et al (1998) for the current forces in a FPSO one has that

$$F_{X,R}(u, v, 0) = \frac{1}{2}\rho U^2 LT \cdot C_{1C}(\alpha)$$
$$F_{Y,R}(u, v, 0) = \frac{1}{2}\rho U^2 LT \cdot C_{2C}(\alpha) \tag{4}$$
$$N_{Z,R}(u, v, 0) = \frac{1}{2}\rho U^2 L^2 T \cdot C_{6C}(\alpha)$$

the coefficients $\{C_{1C}(\alpha); C_{2C}(\alpha); C_{6C}(\alpha)\}$ being given in terms of the ship main dimensions by the expressions (B = beam; T = draft; L = length; C_B = block coefficient):

$$C_{1C}(\alpha) = C_f(R_e)\cos\alpha + \frac{\pi T}{8L}(\cos 3\alpha - \cos\alpha)$$
$$C_{2C}(\alpha) = \left(C_Y - \frac{\pi T}{2L}\right)\sin\alpha|\sin\alpha + \frac{\pi T}{2L}\sin^3\alpha + \frac{\pi T}{2L}\left(1 + 0.4\frac{C_B B}{T}\right)\sin\alpha|\cos\alpha| \tag{5}$$
$$C_{6C}(\alpha) = -lC_Y \sin\alpha|\sin\alpha| - \frac{\pi T}{L}\sin\alpha\cos\alpha - \frac{\pi T}{2L}\left(\frac{1 + |\cos\alpha|}{2}\right)^2\left(1 - 4.8\frac{T}{L}\right)\sin\alpha|\cos\alpha|$$

As anticipated, the parcel that depends on (u, v) depends only on three hydrodynamic coefficients: the friction coefficient C_f(Re), the cross-flow drag coefficient C_Y, and the cross-flow moment coefficient[2] lC_Y. Using the ITTC friction-line with factor of form $(1 + k)$, see van Manem & van OOssanen (1988), and observing that S is the wetted surface, one has

$$C_f(R_e) = \frac{0.075}{(\log_{10} R_e - 2)^2} \cdot \frac{S}{TL}(1 + k) \tag{6}$$

The value of the factor k depends on the hull form and on Froude number. One could use, as a first approximation, experimental values presented in literature for similar ships. Van Manem & van Oossanen (1988), for example, present the Prohaska correction for a methane carrier and obtain the near zero Froude value of $k = 0.25$. Leite (1997) estimated $k = 0.39$ for a VLCC hull in full-load condition based on experimental results presented by Wichers (1988).

[2]Here l represents the longitudinal distance between the origin of the local coordinate system (mid-ship section) and the center of pressure for beam incidence.

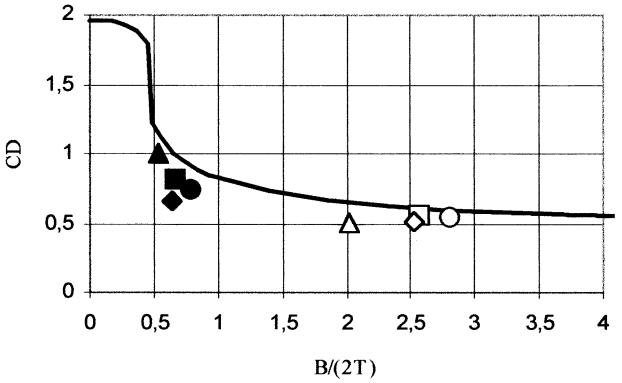

Fig. 1 Hoerner's curve for C_D and experimental values from Table 2.1. (black spots = loaded; white spots = ballasted 40%)

The cross-flow coefficient C_Y can be estimated from Hoerner's curves for the drag coefficient C_D on rectangles, see Hoerner (1965); as it is known, C_D is a function of both $B/2T$ and the section bilge radius and taking the lowest of these curves, to account for some three dimensional effect, one has the curve shown in Fig. 1.

In Table 1 the experimentally determined values of $\{C_Y; lC_Y\}$, for different ship models, are listed. The values of C_Y have been plotted in Fig. 1 for the sake of comparison. The agreement is not bad and Hoerner's curve can be used at least in a first approximation.

The experimental values corresponding to the moment coefficient lC_Y, however, present a great variability and one could not detect a trend either with B/L or with $B/2T$. Since the influence of such a parcel should be relatively small, one can use the average value $lC_Y = 0.035$ in the simulations. Nevertheless, it is important to observe that such an assumption implies somewhat large discrepancies, especially concerning VLCC2 results. Assuming this average value, together with (6) and Hoerner's curve of Fig. 1, the hydrodynamic model becomes explicit, in the sense that the horizontal generalized forces can be estimated from the main ship dimensions.

Rotation test $(u = v = 0)$

A simple experimental set up is the "rotation test," where a uniform yaw velocity is imposed to the model and the yaw moment $\Delta N_Z(0, 0, r)$ is measured. The dependence between the moment

Table 1 Experimental values of cross-flow coefficients $\{C_Y; lC_Y\}$

SYMBOL	SHIP	LAB.	%T	C_B	B/L	B/2T	C_Y	lC_Y
σ	SHIP1	IPT	100%	0.82	0.11	1.02	1.00	0.014
Δ	SHIP1	IPT	40%	0.77	0.11	2.55	0.50	0.043
•	SHIP2	IPT	100%	0.82	0.17	1.37	0.70	0.048
○	SHIP2	IPT	40%	0.77	0.17	3.44	0.54	0.028
■	VLCC1	IPT	100%	0.83	0.17	1.26	0.87	0.045
□	VLCC1	IPT	40%	0.77	0.17	3.16	0.52	0.050
♦	VLCC2	MARIN	100%	0.85	0.15	1.25	0.68	0.004
◊	VLCC2	MARIN	40%	0.83	0.15	3.12	0.49	0.005
								0.035

Table 2 Experimental values of $32C_{6,rr}/C_Y$ in rotation test (IPT). (C_Y determined from Hoerner's curve, see Fig. 1)

SHIP	%T	C_B	B/L	B/2T	C_Y	$32C_{6,rr}/C_Y$
SHIP2	100%	0.82	0.17	1.37	0.75	2.16
SHIP2	40%	0.77	0.17	3.44	0.56	1.86
VLCC1	100%	0.83	0.17	1.26	0.78	1.99
VLCC1	40%	0.77	0.17	3.16	0.57	1.88
						2.0

and the yaw velocity should be of the form

$$\Delta N_Z(0,0,r) = -\frac{1}{2}\rho TL^4 \cdot C_{6,rr} \cdot |r|r \tag{7}$$

A strict linear dependence between the measured moment and r^2 has been observed in all experiments and it is expected, certainly, that the coefficient $C_{6,rr}$ must increase with C_Y. The experimental result, shown in Table 2, gives some support to this expectation since the relation $32\ C_{6,rr}/C_Y = 2.0$ is roughly satisfied in all cases tested with an error smaller than 10%. This relation has been assumed in the derivation of the proposed hydrodynamic model.

Cross-flow

The sectional cross-flow coefficient changes along the ship axis, a typical figure being presented, for example, by Faltinsen (1990). Such coefficient distribution, after multiplied by a reduction factor (also extracted from Faltinsen (1990)) in order to account for some three-dimensional effects, has been adopted as a model and denoted $C_{D,FALT.}(x)$ in the present work. The cross-section coefficient was then re-normalized in order to recover the global cross-flow coefficients C_Y and lC_Y; in this way, the following form for the sectional drag coefficient $C_D(x)$ has been assumed:

$$C_D(x) = C_{D,FALT.}(x) \cdot f_1(x) \cdot f_2(x) \tag{8}$$

the weighting functions $f_j(x)$ depending on two parameters (see Fig. 2) are determined from the equalities

$$\begin{aligned} \frac{1}{L}\int_{-L/2}^{L/2} C_D(x)\,dx &= C_Y \\ \frac{1}{L_2}\int_{-L/2}^{L/2} xC_D(x)\,dx &= lC_Y \end{aligned} \tag{9}$$

Figure 2 presents the weighting functions $f_j(x), C_{D,FALT.}(x)$ and $C_D(x)$ for VLCC1 in full-load (100%) condition.

The sectional drag force can then be expressed as

$$f_y(x) = -\frac{1}{2}\rho C_D(x)T \cdot \text{sign}(v+rx) \cdot (v+rx)^2$$

and introducing the coefficients (see Simos et al (1998))

$$\begin{aligned} &I_j(v,r) \\ &= \frac{1}{L^{j+1}}\int_{-L/2}^{L/2} C_D(x) \cdot \text{sign}(v+rx) \cdot x^j dx;\ j = 0,1,2,3 \end{aligned} \tag{10}$$

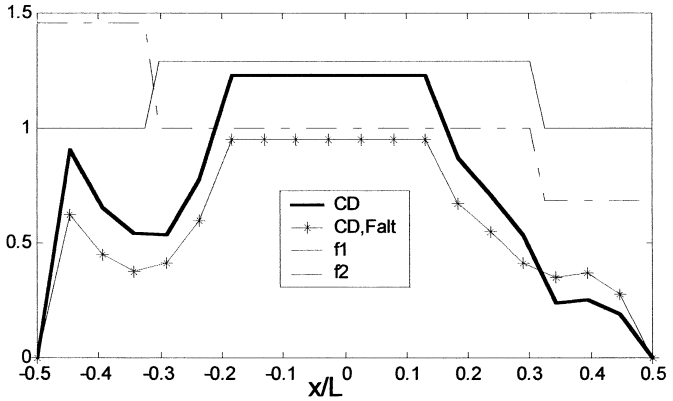

Fig. 2 Weighting functions $f_j(x), C_{D,FALT.}(x)$ and $C_D(x)$ for VLCC1 in full-load (100%) condition

one obtains (see (7) and Table 2)

$$\begin{aligned} \Delta F_{Y,R}(0,v,r) &= -\frac{1}{2}\rho TL \cdot [I_0(v,r) \cdot v^2 - C_Y \cdot v|v|] \\ &\quad -\rho TL^2 \cdot I_1(v,r) \cdot vr - \frac{1}{2}\rho TL^3 \cdot I_2(v,r) \cdot r^2 \\ \Delta N_{Z,R}(0,v,r) &= -\frac{1}{2}\rho TL^2 \cdot [I_1(v,r) \cdot v^2 + lC_Y \cdot v|v|] \\ &\quad -\rho TL^3 \cdot I_2(v,r) \cdot vr - \frac{1}{2}\rho TL^4 \\ &\quad \cdot \left[(I_3(v,r) - I_3(0,r)) \cdot r^2 + \frac{C_Y}{16}|r|r \right] \end{aligned} \tag{11}$$

Note that the parcels proportional to $v|v|$ are already incorporated in (4) (see also (9)) and, therefore, had to be subtracted from the yaw-motion-induced cross-flow results. Also, in the expression for the moment the result from the "rotation test" has been enforced, by subtracting the parcel $I_3(0,r) \cdot r$ and adding (7) in the last term within brackets.

Short wing theory

Using the short wing theory for a flat plate the following coupling forces between surge and yaw velocities can be determined:

$$\begin{aligned} \Delta F_{Y,R}^{(SW)}(u,0,r) &= \frac{1}{4}\rho\pi T^2 L \cdot ur \\ \Delta N_{Z,R}^{(SW)}(u,0,r) &= -\frac{1}{8}\rho\pi T^2 L^2 \cdot |u|r \end{aligned}$$

In a flat plate with constant draft, the lateral force has the sign of the velocity u but the moment depends on $|u|$. To verify this result it is sufficient to consider the coordinated system $x_1 = -x; y_1 = -y$ while the plate is displaced with velocity $u_1 = -u; v_1 = -v; r_1 = r$. Using now the analytical approximations proposed by Clarke et al (1982) for the linear derivatives $\{Y_r; N_r\}$, but subtracting from them the inertia terms already

Table 3 Parameters of tested models—full-scale dimensions ($\lambda = L_{FULL}/L_{MODEL}$; C_Y = cross-flow coefficient from Hoerner's curve)

	SHIP2-100%	SHIP2-40%	VLCC1-100%	VLCC1-40%	VLCC2-100%	VLCC2-40%
M(kg)	1.563×10^{8}	0.587×10^{8}	3.219×10^{8}	1.117×10^{8}	2.406×10^{8}	0.911×10^{8}
$\mathbf{I_Z}$(kg.m^2)	0.66×10^{12}	0.250×10^{12}	2.060×10^{12}	0.720×10^{12}	1.520×10^{12}	0.651×10^{12}
$\mathbf{M}_{11}$(kg)	0.851×10^{7}	0.156×10^{7}	1.848×10^{7}	0.254×10^{7}	1.562×10^{7}	0.245×10^{7}
$\mathbf{M}_{22}$(kg)	1.420×10^{8}	0.241×10^{8}	2.725×10^{8}	0.353×10^{8}	2.459×10^{8}	0.527×10^{8}
$\mathbf{M}_{66}$(kg.m^2)	0.472×10^{12}	0.089×10^{12}	1.579×10^{12}	0.222×10^{12}	1.210×10^{12}	0.229×10^{12}
$\mathbf{M}_{26}$(kg.m)	0.809×10^{9}	0.171×10^{9}	2.209×10^{9}	0.353×10^{9}	0.803×10^{9}	0.339×10^{9}
L(m)	260	260	320	320	310	310
T(m)	16.1	6.44	21.47	8.63	18.90	7.56
B(m)	44.5	44.5	54.5	54.5	47.17	47.17
$\mathbf{x}_G$(m)	7.41	7.18	9.81	4.44	6.6	6.6
S(m^2)	1.764×10^{4}	1.174×10^{4}	2.734×10^{4}	1.791×10^{4}	2.280×10^{4}	1.390×10^{4}
$\mathbf{C_B}$	0.818	0.77	0.83	0.76	0.85	0.80
$\mathbf{C_Y}$	0.70	0.54	0.87	0.52	0.68	0.49
$l\mathbf{C_Y}$	0.048	0.028	0.045	0.050	0.004	0.005
λ	70	70	90	90	82.5	82.5

present in (1), one obtains

$$\begin{aligned}&\Delta F_{Y,R}(u,0,r)\\&\quad=\frac{1}{4}\rho\pi T^2L\cdot\left(1-4.4\frac{B}{L}+0.160\frac{B}{T}\right)\cdot ur+M_{11}\cdot ur\\&\Delta N_{Z,R}(u,0,r)\\&\quad=-\frac{1}{8}\rho\pi T^2L^2\cdot\left(1+0.16\frac{B}{T}-2.2\frac{B}{L}\right)\cdot|u|r+M_{26}\cdot ur\end{aligned}\tag{12}$$

To derive the influence of the yaw velocity on the surge force some results from the short wing theory are recalled here. In fact, for $u \gg (v; rL/2)$ one has the classical Jones expression (see Jones (1946))

$$C_L=\frac{F_Y^{(SW)}}{1/2\rho u^2LT}=\frac{\pi A}{2}\alpha_a$$

$$\alpha_a=-\frac{v}{u}+\frac{rL}{2u}$$

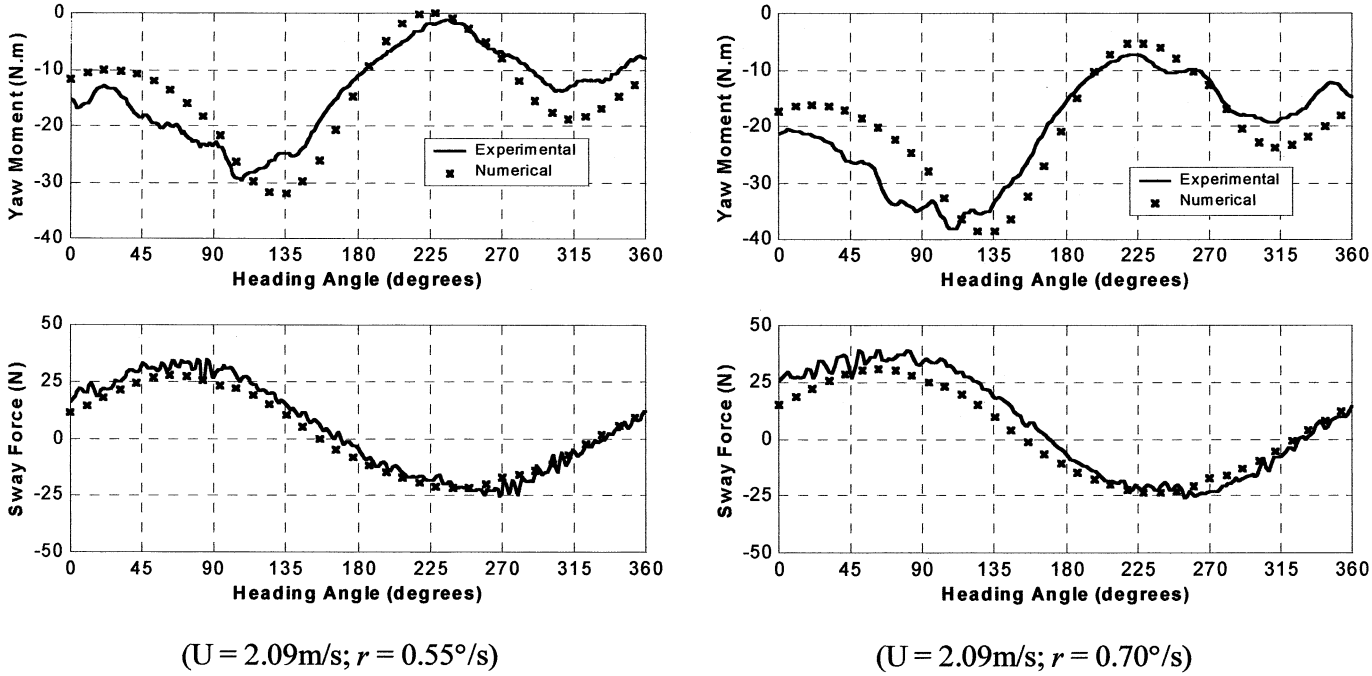

Fig. 3 SHIP2-100%: results from yaw rotating tests

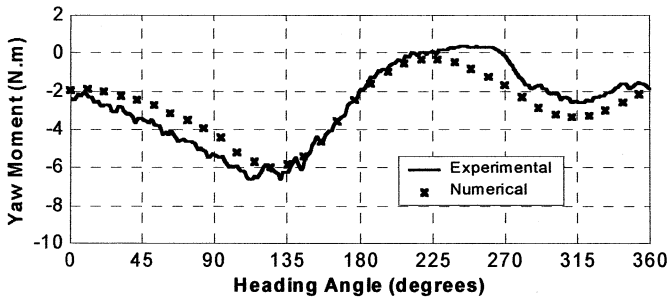

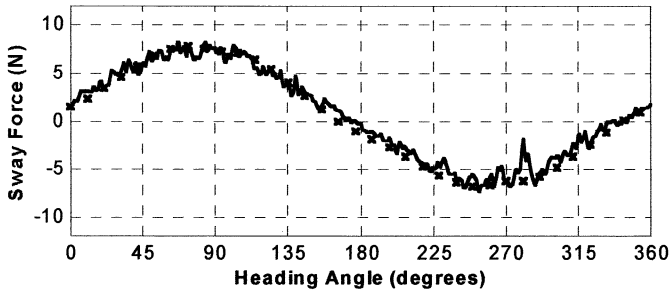

(U = 2.09m/s; r = 0.37°/s)

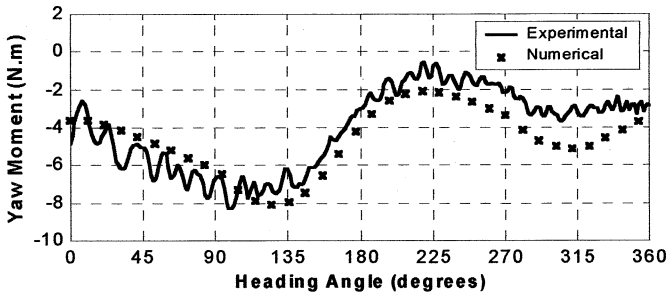

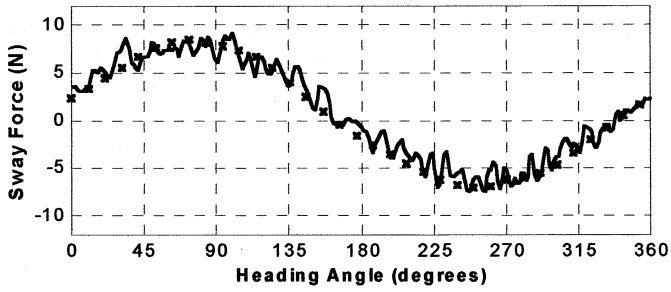

(U = 2.09m/s; r = 0.55°/s)

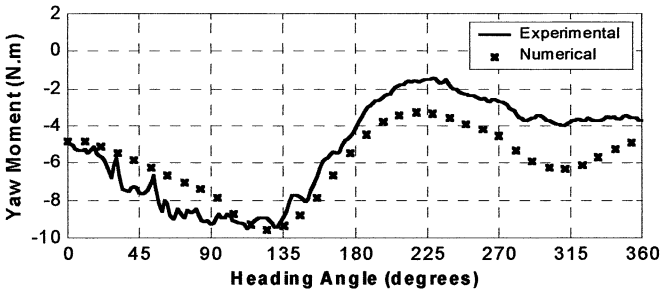

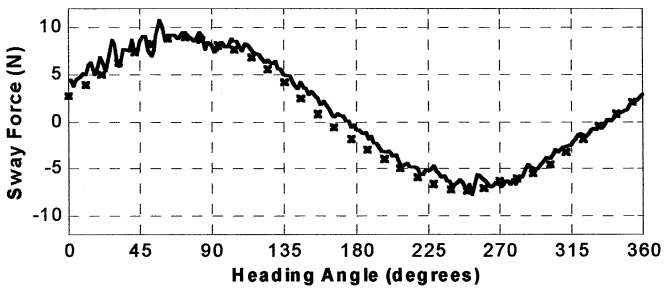

(U = 2.09m/s; r = 0.66°/s)

Fig. 4 SHIP2-40%: results from yaw rotating tests

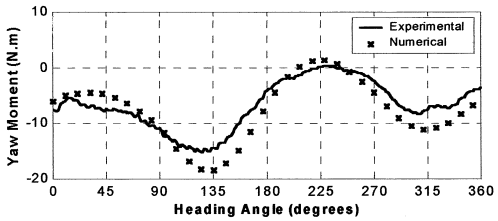

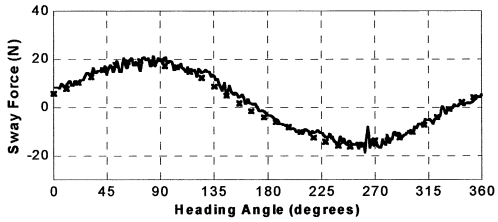

(U = 1.90m/s; r = 0.33°/s)

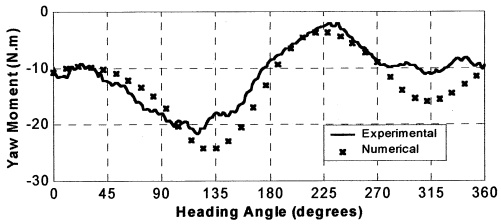

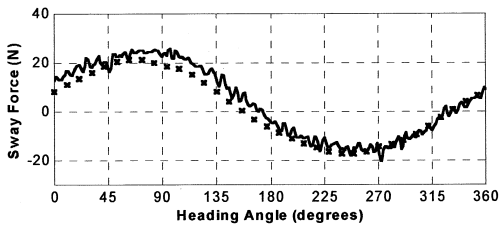

(U = 1.90m/s; r = 0.48°/s)

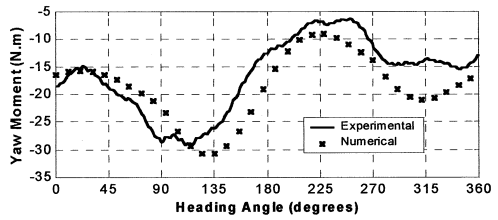

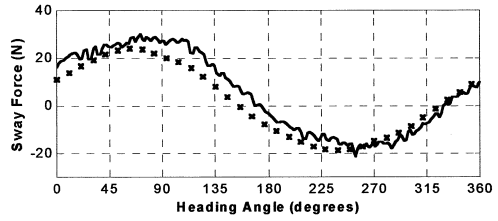

(U = 1.90m/s; r = 0.62°/s)

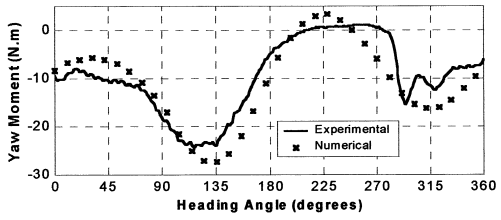

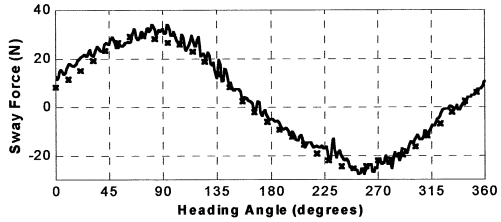

(U = 2.37m/s; r = 0.38°/s)

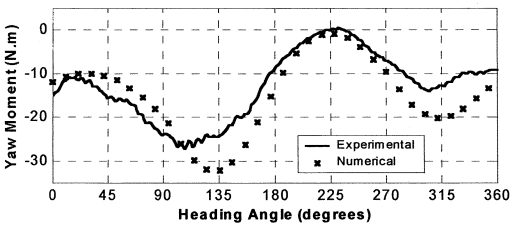

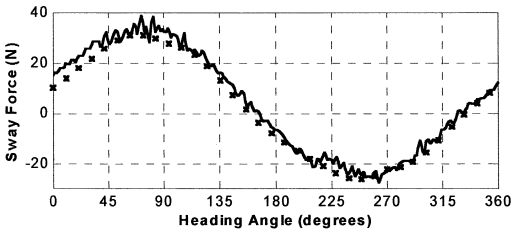

(U = 2.37m/s; r = 0.48°/s)

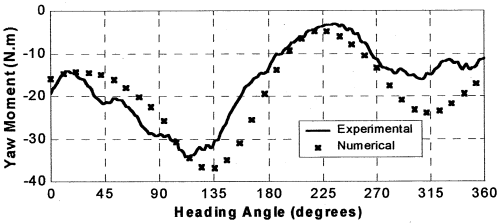

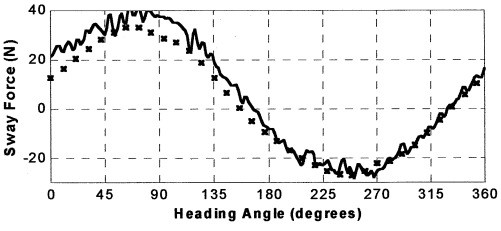

(U = 2.37m/s; r = 0.58°/s)

Fig. 5 VLCC1-100%: results from yaw rotating tests

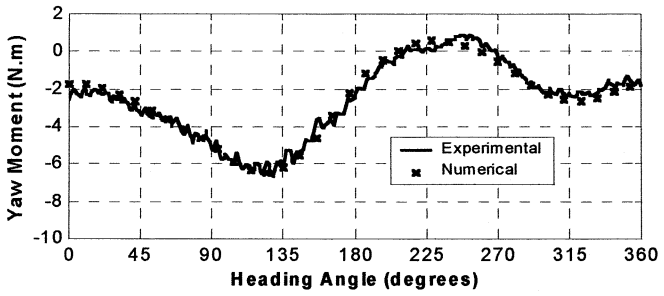

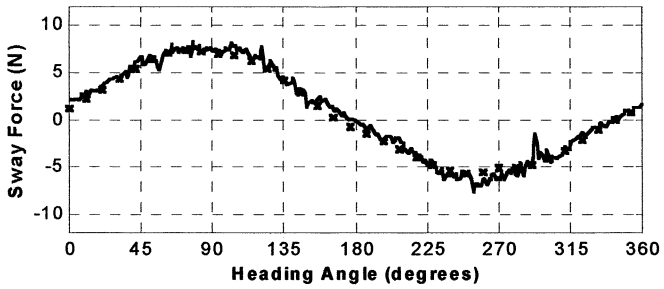

(U = 2.37m/s; r = 0.33°/s)

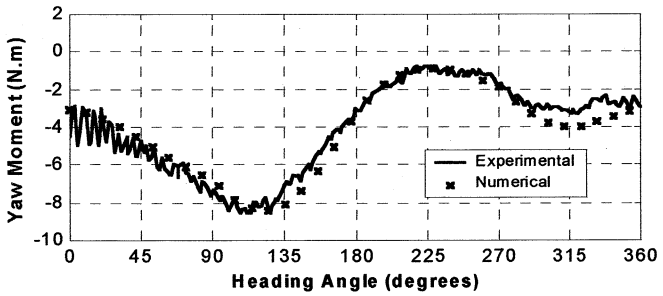

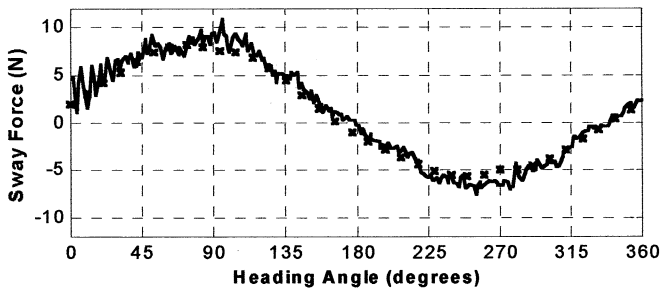

(U = 2.37m/s; r = 0.49°/s)

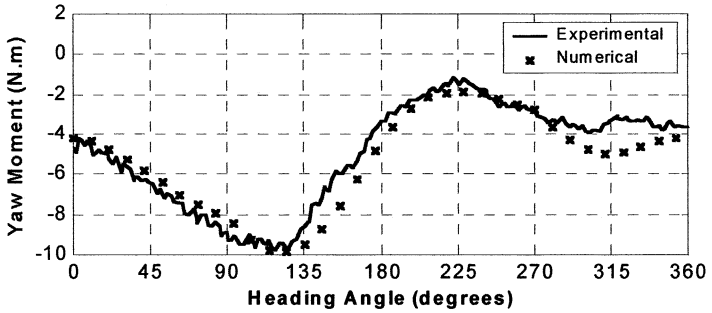

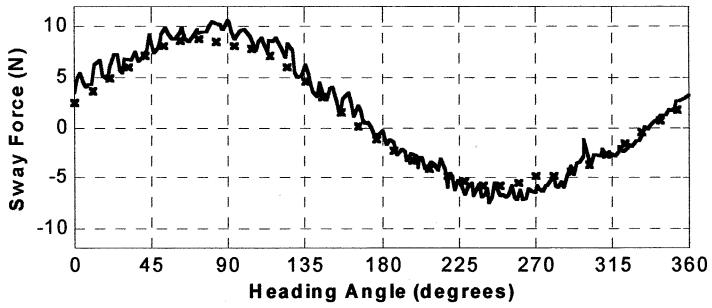

(U = 2.37m/s; r = 0.58°/s)

Fig. 6 VLCC1-40%: results from yaw rotating tests

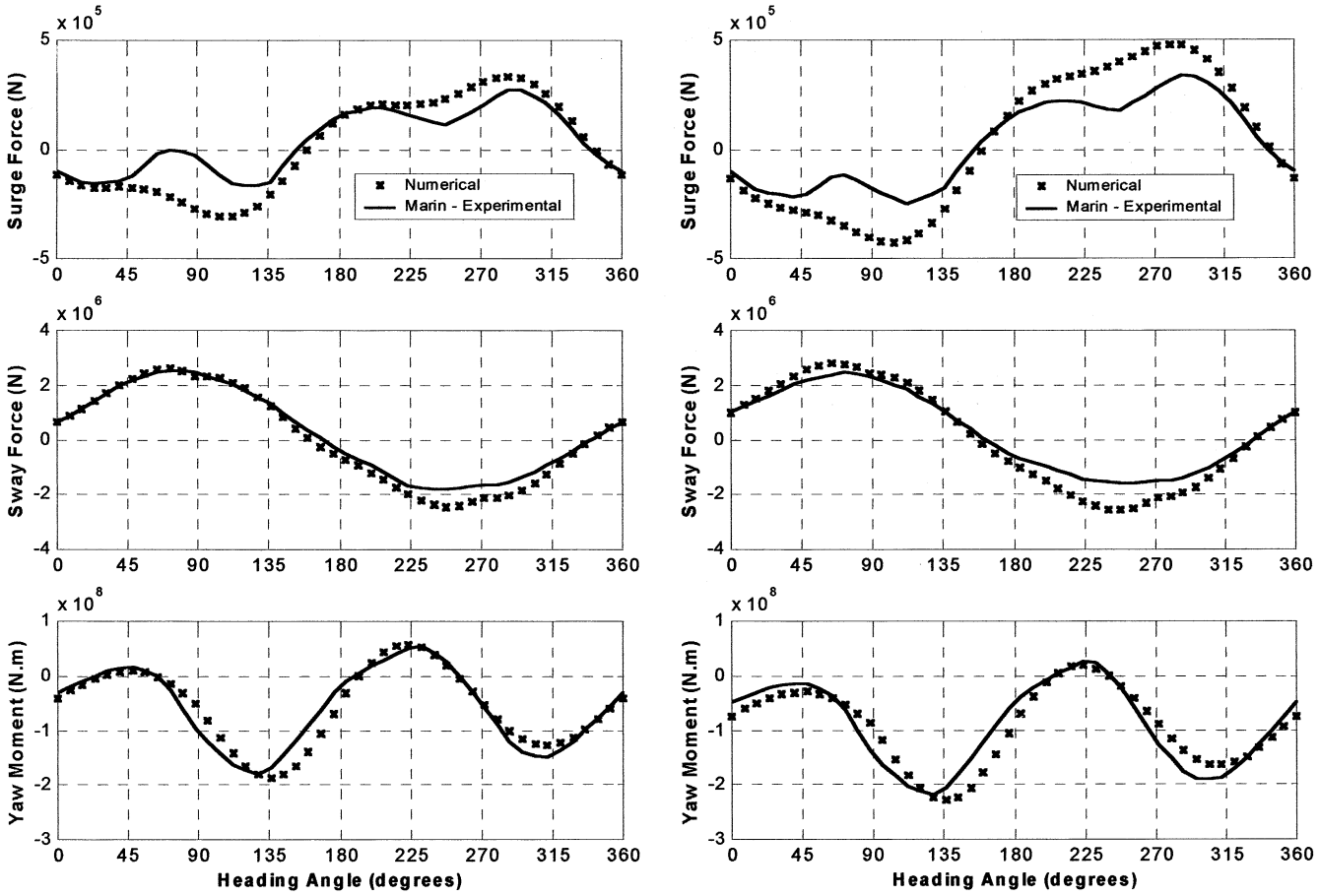

Fig. 7 VLCC2-100%: results from yaw rotating tests

where α_a is the angle off attack and $A = 2T/L$ is the aspect ratio. The induced drag is then given by

$$C_D = \frac{C_L^2}{\pi A} = \frac{\pi T}{2L}\left(-\frac{v}{u} + \frac{rL}{2u}\right)^2$$

Expanding the above expression and recalling that $M_{22} = 1/2\rho\pi T^2 L$ for a flat plate, the following expression for the surge force can be derived:

$$F_X^{(SW)} = -\frac{1}{2}\rho u^2 LT \cdot C_D = -\left(\frac{1}{4}\rho\pi T^2 \cdot v^2 + \frac{1}{4}\rho\pi T^2 L \cdot vr + \frac{1}{16}\rho\pi T^2 L^2 \cdot r^2\right) + M_{22} \cdot vr$$

Since the inertia parcel $M_{22} \cdot vr$ is already present on the left side of (1) and $M_{26} = 0$ for a flat plate one obtains, observing that the term proportional to v^2 has already been incorporated in (4), that

$$\Delta F_{X,R}(u, v, r) = -\frac{1}{4}\rho\pi T^2 L \cdot vr - \frac{1}{16}\rho\pi T^2 L^2 \cdot r^2; \quad u \gg (v; rL/2)$$

The idea from now on is that, in the above expression, the hydrodynamic derivatives are well represented for α_a small and could, in this way, be extended to arbitrary values of the arguments assuming the function to be analytic. There remains one problem, however, related with the parcel proportional to r^2: a symmetry argument shows that, for a flat plate, this parcel should be an odd function of u; this could be corrected if it is observed that, for a fixed value of $(-v + rL/2)$, the number $\cos[a\tan(-v/u + rL/2u)]$ has the sign of u. The following expression is then proposed:

$$\begin{aligned} \alpha_a &= a\tan(-v/u + rL/2u) \\ \Delta F_{X,R}(u, v, r) &= -\frac{1}{4}\rho\pi T^2 L \cdot vr - \frac{1}{16}\rho\pi T^2 L^2 \cdot \cos\alpha_a \cdot r^2 \end{aligned} \tag{13}$$

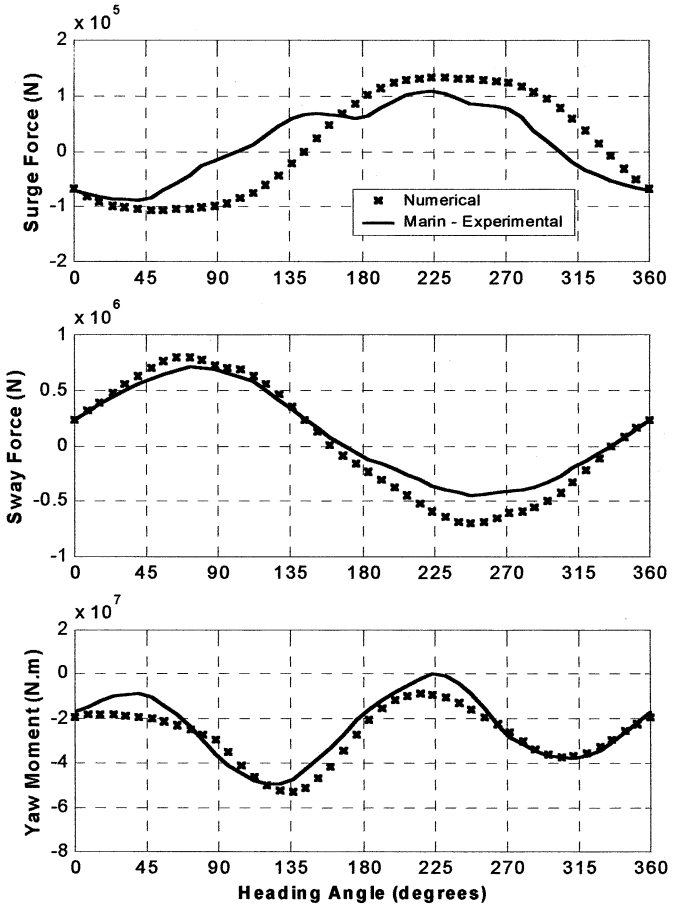

$(U = 1.03\text{m/s}; r = 0.17°/\text{s})$

Fig. 8 VLCC2-40%: results from yaw rotating tests

Summarizing: with $\{F_{X,R}(u,v,0); F_{Y,R}(u,v,0); N_{Z,R}(u,v,0)\}$ defined in (4), $\{\Delta F_{Y,R}(0,v,r); \Delta N_{Z,R}(0,v,r)\}$ defined in (11), $\{\Delta F_{Y,R}(u,0,r); \Delta N_{Z,R}(u,0,r)\}$ defined in (12) and $\Delta F_{X,R}(u,v,r)$ defined in (13), the generalized fluid forces in (1) can be expressed as:

$$\begin{aligned} F_{X,R}(u,v,r) &= F_{X,R}(u,v,0) + \Delta F_{X,R}(u,v,r) \\ F_{Y,R}(u,v,r) &= F_{Y,R}(u,v,0) + \Delta F_{Y,R}(u,0,r) \\ &\quad + \Delta F_{Y,R}(0,v,r) \\ N_{Z,R}(u,v,r) &= N_{Z,R}(u,v,0) + \Delta N_{Z,R}(u,0,r) \\ &\quad + \Delta N_{Z,R}(0,v,r) \end{aligned} \tag{14}$$

Assuming, as it is reasonable at least in a first approximation, that the cross-flow coefficients $\{C_Y; lC_Y; I_j(v,r), j = 0,1,2,3\}$ are weakly dependent on the Reynolds number Re, and that the same assumption can be made about the coefficients from the short wing theory, only one coefficient remains scale-dependent: the friction coefficient $C_f(\text{Re})$. However, as discussed in the accompanying paper, this scale dependence is crucial in the analysis of the fishtailing instability.

The hydrodynamic model (14) is quasi-explicit, in the sense that it depends on the ship's main dimensions and on only three hydrodynamic coefficients: $C_f(\text{Re})$, C_Y and lC_Y. Furthermore, as discussed earlier in the sway and surge components section, these coefficients may even be reasonably well estimated by some standard results in fluid mechanics and ship hydrodynamics.

In the next section the fluid forces (14) are compared with the ones measured both at IPT and Marin's wave tank, in a class of experiments known as the "yaw rotating test." The important question of the *robustness* of (1) and (14), namely, the ability of the model to correctly predict some relevant and more complicated dynamic phenomenon, such as the fishtailing instability, for example, is addressed in the aforementioned companion paper.

3. Experimental results—yaw rotating test

In the *yaw rotating test* the ship's model, scaled accordingly to Froude's law, is towed with uniform velocity U in the longitudinal wave tank direction, while rotating with constant yaw angular velocity r. The forces in the horizontal plane are then measured, together with the yaw moment, and can be compared to the forces $\{F_X; F_Y; N_Z\}$ obtained from (1) and (14) when $\{u(t) = U \cdot \cos(rt); v(t) = -U \cdot \sin(rt)\}$ and the yaw velocity is constant r. The Reynolds number is defined by $\text{Re} = UL/\nu$ and Table 3 gives the main parameters of the tested models.

In all cases the experimental values of the parameters were used. The experimentally determined values of these coefficients are given in Table 1. Later, the "averaged" value $lC_Y = 0.035$ will be assumed and also the cross-flow coefficient C_Y taken from Hoerner's curve of Fig. 1 in order to check the predictive ability of the "explicit" model and, as will be seen, a reasonably close agreement between the results of the yaw rotating tests and the mathematical model is observed even if the estimated values of the parameters are used instead.

For the IPT results, related to SHIP2 and VLCC1, the sway force and the yaw moment are presented at the small-scale model dimension and the surge force was not measured; the results of VLCC2, obtained at Marin (see Wichers (1987)), are presented in full-scale dimension. In all cases both the velocity U and the angular velocity r are given in full-scale dimension, covering the range $\{1.03\ \text{m/s} \le U \le 2.37\ \text{m/s};\ 0.11\,\text{deg}/s \le r \le 0.70\,\text{deg}/s\}$.

In Figs. 3 and 4 the results from SHIP2 are presented, both at the loaded (100%) and ballasted (40%) conditions; similar results for VLCC1 are shown in Figs. 5 and 6 and for VLCC2 in Figs. 7 and 8. In all tests, the instrumentation precision is approximately $\pm 1N$ for sway force and $\pm 1N$.m for yaw moment measurement.

The observed agreement is in general good for the *sway force*. For the *yaw moment* the concordance is slightly worse, the experimental values from IPT showing some irregularities. It must be observed that a reasonable agreement persists even for high values of the angular velocity, around 0.70 deg/s in full-scale. Finally, the results for the *surge force* (see Figs. 7 and 8) are just fair, reflecting obvious problems in its theoretical representation (especially concerning its wing component for high values of the angle of attack) and, possibly, also some experimental difficulties in the measurement of such small force.

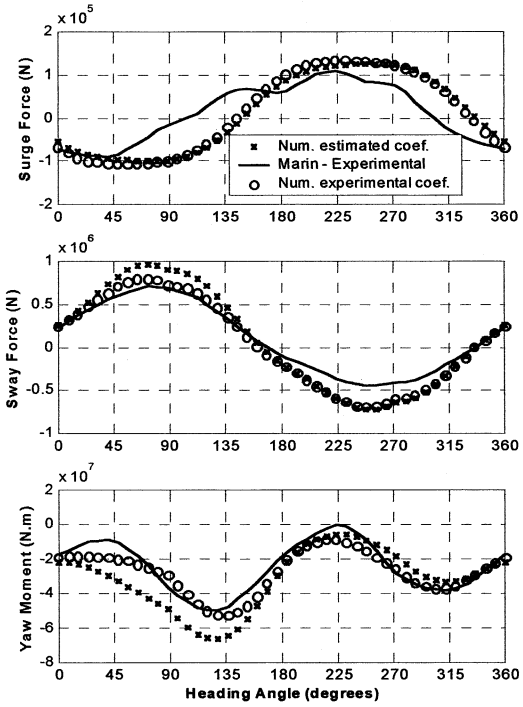

(VLCC2; 40%; U = 1.03m/s; r = 0.17°/s)

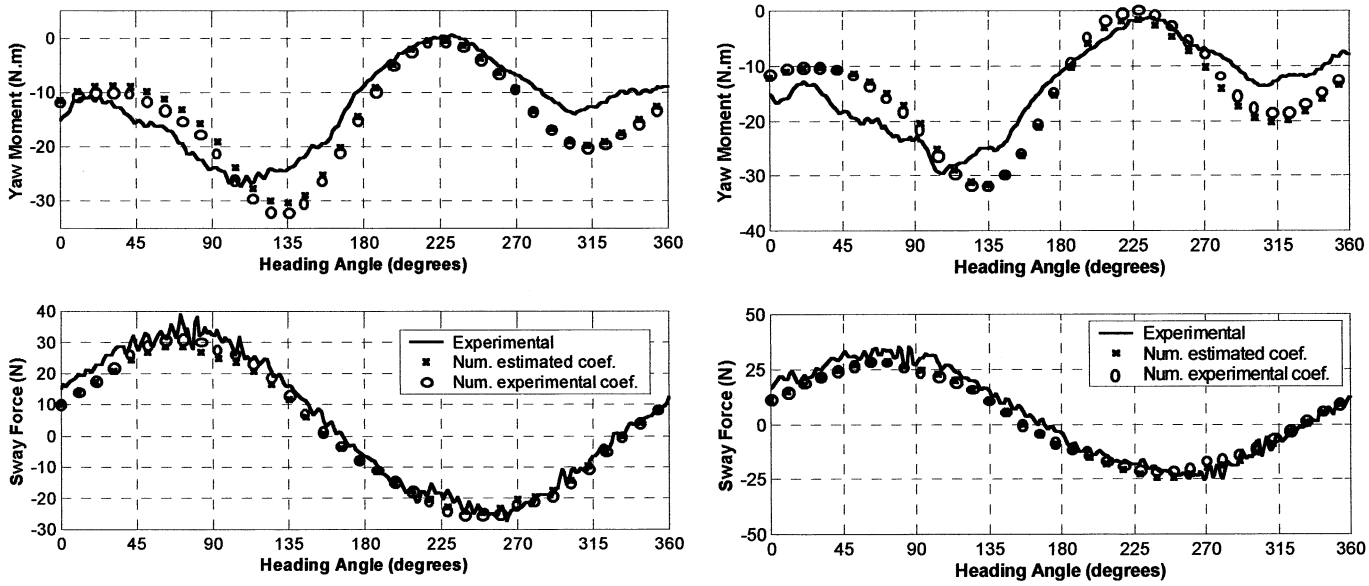

(*VLCC1 – 100%*; U = 2.37m/s; r = 0.48°/s)

(*SHIP2 – 100%*; U = 2.09m/s; r = 0.55°/s)

Fig. 9 Comparison between "quasi-explicit" and "explicit" models

Figure 9 reproduces some of the cases discussed above for the different models tested, but with the numerical results also computed with the estimated values of the hydrodynamic parameters: friction coefficient $C_F = 0.050$, estimated from equation (6) with $k = 0.39$ for the VLCC2 case and cross-flow coefficients estimated from Hoerner's curve of Fig. 1 $\{C_Y = 0.75(\text{SHIP2; } 100\%); 0.78(\text{VLCC1; } 100\%); 0.57(\text{VLCC2; } 40\%)\}$ and by the average value of the moment coefficient $lC_Y = 0.035$. It can be readily seen that there is indeed a better agreement with the yaw rotating measurements when the experimental values of the coefficients are adopted in the simulations, as should be expected. It must be noted, however, that the numerical results of sway force obtained with estimated parameters can hardly be distinguished from those obtained when all the parameters are effectively measured in model-scale tests. For the yaw moment, the discrepancies are also relatively small, unless for the VLCC2 results. The higher discrepancies observed in this case are due to the large difference between the average value of $lC_Y = 0.035$ adopted and its experimentally determined value $lC_Y = 0.005$. The relatively good agreement between numerical predictions and experiments suggests that a "explicit" version of the model could indeed be suitable for a first approximation. However, given the uncertainties involved in the estimation of the moment coefficient, it would be advisable to consider a certain variation of the lC_Y parameter. For tankers, experimental results from Table 1 indicate that such a coefficient should typically be in the range $0 \leq lC_Y \leq 0.05$.

Finally, as discussed before, the only scale effect in the present hydrodynamic model is related to the friction coefficient $C_f(\text{Re})$ that appears in the surge force. The results shown in Fig. 7 refer to the friction coefficient at the model scale and Fig. 10 shows the surge force computed both at model and full scales. Despite the large difference between the friction coefficients in the two cases ($C_{f,MODEL} = 3.31 \times C_{f,FULL}$), the remaining terms in the equation (1) depend exclusively on the geometry and main ship dimensions and they apparently dominate the final value of the surge force. At first sight, then, the scale-effect is of secondary importance and could eventually be ignored in the study of a moored FPSO.

As shown in the accompanying paper, however, the fishtailing phenomenon depends crucially on the value of $C_f(\text{Re})$, a fact that had already been pointed out by other authors (see, for example, Faltinsen (1979) and Jiang & Sharma (1993)): a single-point moored ship behaves essentially as a pendulum, the friction force on the ship's hull (namely, $C_f(\text{Re})$) playing the role of the gravity in the pendulum analogy. In this context, even a small difference in $C_f(\text{Re})$ implies large differences in the response, and the geometry of the fishtailing instability cannot be extrapolated from model scale to full scale. Furthermore, in the fishtailing behavior of a single-point moored system, the heading angle is usually not higher than 20 deg; for such small angles the frictional term in the surge force is indeed dominant and, thus, the difference between the surge forces in real and model scale are significant, as can be seen in Fig. 10. It turns out, then, that adequate representation of the fishtailing phenomenon in full-scale is strongly dependent on the appropriate consideration of viscous effects ($C_f(\text{Re})$).

This observation is important since it helps to clarify some properties of the hydrodynamic model that guided the present choice. First of all, the emphasis on a clear *physical background* is now evident: there is no law that makes it possible to extrapolate the surge force coefficient from model scale to full scale,

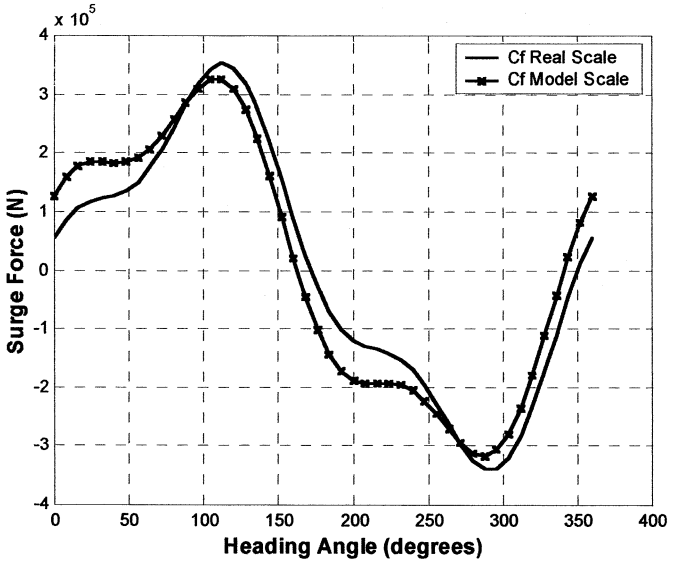

Fig. 10 Surge force for VLCC2-100% ($U = 1.03$ m/s; $r = 0.11$deg/s). (—· × ·—) = model scale; (—· = full scale)

since in the expression of this force a scale-dependent parcel appears together with parcels that are not scale-dependent. Only by means of a physical model can these parcels be separated and extrapolated conveniently. Second, the study of the *robustness* of the model can be better appreciated by singling out a prominent dynamic phenomenon, the fishtailing instability in this case, where one could recognize the sensible parameters and, by contrast, the parameters that are not so essential. In the present case, as shown in the accompanying paper, the friction coefficient $C_f(\text{Re})$ is the sensible parameter in the fishtailing phenomenon while the cross-flow coefficients $\{C_Y; lC_Y\}$ are relatively non-essential, due to the small heading angles involved. In particular, as will be seen, the behavior of the system is essentially the same if $\{C_Y; lC_Y\}$ is obtained directly from experiments, as in Table 1, or inferred from Hoerner's curve, as in Table 3. This feature renders possible the third desirable quality of the proposed model, of being *explicit*, namely, of being able to predict the behavior of the system without the need of an extensive experimental pre-analysis.

To finalize the present work, it seems worthwhile to call the attention to a last point. Because the fishtailing instability depends crucially on $C_f(\text{Re})$ it is hopeless to try to infer the full-scale behavior from the fishtailing behavior of a ship model in a wave tank. Only proper mathematical models can be used as extrapolators, which places on them an extra responsibility. This point is addressed in the accompanying paper, where the mathematical model's ability to cope with the fishtailing instability phenomenon is analyzed.

Acknowledgments

The authors wish to thank PETROBRAS for supporting the tests conducted at IPT. The first and second authors were supported by FAPESP—The State of São Paulo Research Foundation. Finally, the authors want to thank engineer João V. Sparano

for his collaboration. The third and fourth authors also acknowledge the CNPq Research Fund.

References

ARANHA, J. A. P. 1996 Second order horizontal steady forces and moment on a floating body with small forward speed. *Journal of Fluid Mechanics*, **313**, 39–54.

ARANHA, J. A. P. AND MARTINS, M. R. 2000 Low frequency wave force spectrum influenced by wave-current interaction. submitted.

CLARKE, D., GEDLING, F., AND Hine, G. 1982 The application of manoeuvring criteria in hull design using linear theory. *The Royal Institution of Naval Architects*, 45–68.

FALTINSEN, O. M., KJAERLAND, O., LIAPIS, N., AND WALDERHAUG, H. 1979 Hydrodynamic analysis of tankers at single-point-mooring systems. *Proceedings,* 2nd International Conference on Behaviour of Off-Shore Structures, BOSS´79, 177–205.

FALTINSEN, O. M. 1990 *Sea Load on Ships and Offshore Structures*, Cambridge University Press.

HOERNER, S. F. 1965 *Fluid Dynamic Drag*, authors' publication, New Jersey.

JIANG, T. AND SHARMA, S. D. 1993 Maneuvering simulation of a single-point moored tanker in deep and shallow water. *Proceedings*, International Conference on Marine Simulation and Ship Manoeuvrability, MARSIM'93, 229–241.

JONES, R. T. 1946 Properties of low-aspect-ratio pointed wings at speeds below and above the speed of sound. NACA Report 835.

JONES, R. T. AND COHEN, D. 1960 *High Speed Wing Theory Princeton Aeronautical Paperbacks* No. 6, Princeton University Press, Princeton, New Jersey.

KIJIMA, K. 1996 Influence of model scale in the determination of the hydrodynamic derivatives. *Bulletin of the Society of Naval Architects of Japan*, **801/3**, 25–30 (in Japanese).

LEITE, A. J. P. 1997 Current forces on tankers and equilibrium bifurcation of turret systems. Ph.D. thesis, University of São Paulo (in Portuguese).

LEITE, A. J. P., ARANHA, J. A. P., UMEDA, C., AND DE CONTI, M. B. 1998 Current forces in tankers and bifurcation of equilibrium of turret systems: hydrodynamic model and experiments. *Applied Ocean Research*, **20**, 145–156.

VAN MANEM, J. D. AND VAN OOSSANEN, P. 1988 Resistance. *Principles of Naval Architecture* (Second Revision), SNAME, chapter 5, **2**.

OLTMANN, P. AND SHARMA, S. D. 1984 Simulation of combined engine and rudder maneuvers using an improved model of hull-propeller-rudder interactions. *Proceedings*, 15th Symposium on Naval Hydrodynamics, Hamburg, 83–108.

SIMOS, A. N., TANNURI, E. A., AND PESCE, C. P. 1998 Dynamics of a turret-FPSO system and hydrodynamic models. *Proceedings*, 17th International Conference on Offshore Mechanics and Arctic Engineering OMAE'98, Lisbon, Paper OMAE98-410.

WICHERS, J. E. W. 1987 The prediction of the behaviour of single point moored tankers. *Developments in Marine Technology, Floating Structures and Offshore Operations*, **4** November, 125–142.

WICHERS, J. E. W. 1988 A simulation model for a single point moored tanker. Ph.D. thesis, Technical University of Delft.